LUNAR ELECTRIC FIELDS, SURFACE POTENTIAL AND ASSOCIATED PLASMA SHEATHS*

J. W. FREEMAN and M. IBRAHIM
Dept. of Space Physics and Astronomy, Rice University, Houston, Tex., U.S.A.

Abstract. This paper reviews the electric field environment of the Moon. Lunar surface electric potentials are reported as follows:
Solar Wind – Dayside: $\phi_0 + 10$ to $+18$ V
Solar Wind – Terminator: $\phi_0 \sim -10$ to -100 V
Electron and ion densities in the plasma sheath adjacent to each surface potential regime are evaluated and the corresponding Debye length estimated. The electric fields are then approximated by the surface potential over the Debye length. The results are:
Solar Wind – Dayside: $E_0 \gtrsim 10$ V m^{-1} outward
Solar Wind – Terminator: $E_0 \sim 1$ to 10 V m^{-1} inward
These fields are all at least 3 orders of magnitude higher than the pervasive solar wind electric field; however they are confined to within a few tens of meters of the lunar surface.

Any body immersed in a plasma acquires a net negative charge. A body exposed to intense ultra-violet radiation is inclined to acquire a positive charge. The Moon enjoys both of these environments simultaneously. As a result, one expects a complicated surface charge distribution on the lunar surface.

Figure 1 shows the general environment of the Moon. On the left-hand side is shown the continuous flux of photons from the Sun, as well as solar wind protons and electrons. The photon flux dominates the solar wind proton flux and results in the ejection of photoelectrons from the sunlit lunar surface. We expect, therefore, that the dayside will exhibit a positive lunar surface potential. As one progresses towards the terminator regions where the solar wind protons and photons impact the surface at more oblique angles, the solar wind electrons, which have high random velocities, still have free access to the lunar surface with normal incidence. One therefore expects the potential to grow more and more negative as the terminator region is approached. A negative potential at the terminator is predicted.

Figure 2 illustrates these speculations more completely. We see here the positive potential on the dayside surface of the Moon and immediately adjacent to this positive potential, the regions of negative potential generated by the photoelectrons ejected from the lunar surface by the solar ultraviolet photons. This photoelectron sheath contains electron number densities on the order of several thousands to tens of thousands of electrons per cubic centimeter. It is confined to a region within a few meters of the lunar surface.

The surface potential becomes smaller and eventually goes negative as one approaches the terminator region. Above the negative surface potential in the terminator

* Paper presented at the Conference on 'Interactions of the Interplanetary Plasma with the Modern and Ancient Moon', sponsored by the Lunar Science Institute, Houston, Texas and held at the Lake Geneva Campus of George Williams College, Wisconsin, between September 30 and October 4, 1974.

The Moon **14** (1975) 103–114.

region we find a positive ion sheath made up of atmospheric ions. The positive charge regions above the surface may result in part from electron depletion, however, positive ions are seen.

This distribution of charges will give rise to electric fields in the vicinity of the Moon.

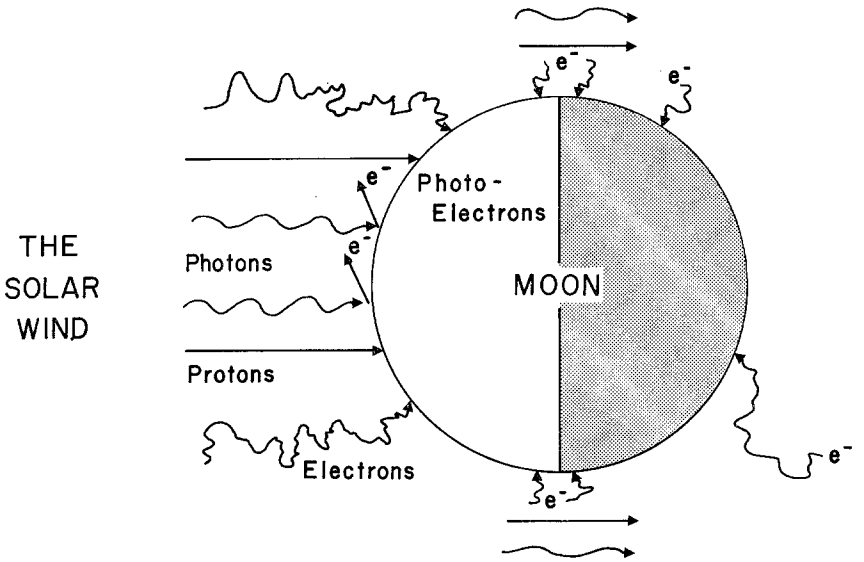

Fig. 1. The solar wind plasma and solar photon environment of the Moon.

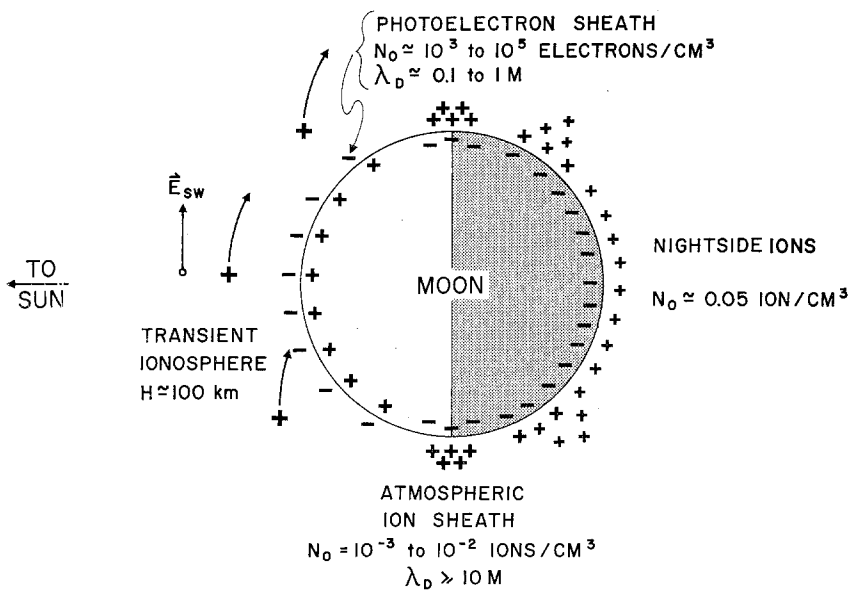

Fig. 2. The electric charge distribution on and near the Moon.

These electric fields will be superimposed on the interplanetary electric field generated by the motion of the solar wind magnetic field past the Moon (The so-called $\mathbf{v} \times \mathbf{B}$ or solar wind electric field). This electric field is approximately 3 orders of magnitude weaker but much more extensive than the electric field associated with the lunar surface potentials. The interplanetary electric field has received considerable attention and will be the subject of several other papers at this conference so the balance of this paper will concentrate on the electric fields associated with the lunar surface potential.

TABLE I

Sunlit lunar surface in the solar wind

Workers	Method	γ	W(eV)	ϕ_0(volts)	$N_0\left(\frac{\text{elect}}{\text{cm}^3}\right)$	$\lambda_D(M)$
Öpik and Singer (1960)	Energy balance			+20 to 25		
Grobman and Blank (1969)	Probe theory	0.001	4	+0.6		
		0.01	6	+10.2		
Manka (1973)	Current balance	$I_p \sim 5 \times 10^{-9}$ amp cm^{-2}		+9		
		$I/10\ I_p$		+4		
Walbridge (1973)	3 Ranges of energy	0.2	6	$\geqslant +3.5$	5×10^3	0.6
					10^5	0.04
Criswell (1973)	Flux balance	0.1 to 0.015	5 to 6	4 to 5 over wide range of conditions		
Feuerbacher *et al.* (1972)	Lunar soils	0.07	5		130	0.78
Reasoner and Burke (1972)	CPLEE Photoelectron Data	0.05	6	Tail data only		

Table I illustrates previous theoretical calculations aimed at determining the dayside lunar electric potential. Öpik and Singer (1960) were the first workers to attempt to estimate the electric potential of the dayside of the Moon. Their results, based on energy balance considerations, indicated potentials on the order of +20 to +25 V. More recently, Grobman and Blank (1969) using collisionless probe theory estimated a range of potentials from approximately +10 V down to practically zero depending on the assumed values for the photoelectric electron yield function and the work function of the lunar surface materials. Manka (1973) carried out similar calculations based on current balance. He found potentials ranging from approximately +4 V to +9 V positive depending again on assumptions about the photoelectron yield function. In a more elaborate calculation, Walbridge (1973) divided the photon flux from the Sun into 3 energy ranges. He found three corresponding electron energy distributions giving a surface potential or the order of +3.5 V or greater for the dayside of the Moon. Criswell (1973) has emphasized the importance of using detailed solar spectra and finds the Lyman alpha photoelectrons to be of significance in stabilizing the day-

side surface potential to a value of approximately 5 V over a wide range of solar photon and particle flux and zenith angle.

Since all of these theories depend explicitly on the photoelectric yield function and the work function of the surface, Feuerbacher *et al.* (1972) undertook to make measurements of these functions on actual lunar soil materials. Their results indicated 0.07 for the photoelectron yield function and 5 eV for the work function. Reasoner and Burke (1972) using data from the CPLEE experiment were able to make in situ estimates of the work function and the photoelectric yield. Their data, which were taken when the Moon was in the geomagnetic tail, indicate values for both of these numbers, in rough agreement with those of Feuerbacher *et al.* Based on this, the lower limit for the surface potential given by Grobman and Blank is inapplicable and the predicted lunar surface potentials range in value from few volts to 25 V positive.

Experimental values for the lunar surface potential have been obtained by the Apollo lunar surface suprathermal ion detector experiment (SIDE) (Freeman *et al.*, 1973). Figure 3 illustrates the configuration of the SIDE as deployed on the lunar surface. Immediately beneath the SIDE instrument is a ground plane electrode. This

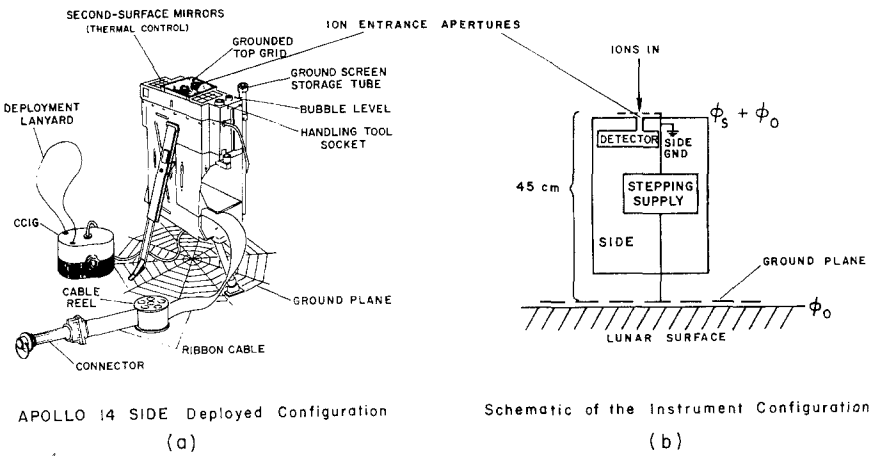

Fig. 3. The mechanical and schematic details of the deployed SIDE.

ground plane electrode is wired to a stepping supply inside the SIDE detector, which is in turn referenced to the SIDE ground. A small wire mesh grid immediately above the input aperture for the ion detectors is also wired to SIDE ground. Through this stepping supply it is possible to alter the electric potential of the SIDE instrument relative to the lunar surface. When the stepping supply is negative, ions generated in the lunar atmosphere by solar ultraviolet and ionization from the solar wind can be accelerated directly into the instrument and the energy with which they are detected will be given by Equation (1); assuming of course that the lunar surface is positive,

$$\varepsilon/q = \varepsilon_i/q - (\phi_0 + \phi_s)\,, \tag{1}$$

where ε is the detection energy; ε_i, the ion initial energy; ϕ_0 and ϕ_s, the lunar surface

potential and stepping supply potentials, respectively; and q is the ion charge (assumed to be unity). The SIDE actually measures energy per unit charge in 20 discrete differential steps from 10 eV q^{-1} to 3500 eV q^{-1} for positive ions. The ground plane stepper has 23 discrete voltage levels. See Freeman *et al.* (1973) for a table of measurable lunar surface potentials.

We note the assumption that the initial energy of the ions is negligible compared to the energy acquired by acceleration by the instrument and the lunar surface potential. The initial energy of the ions is the thermal energy of the neutral atoms from which they originated. The assumption of negligible energy is therefore justified. However, if the initial energy is nonnegligible the calculated values for the lunar surface potential represent lower limits.

As the SIDE steps through various energy channels and ground plane stepping voltages 'resonances' occur which consist of enhanced detector response in the energy channels appropriate to the instantaneous lunar surface potential for each ground

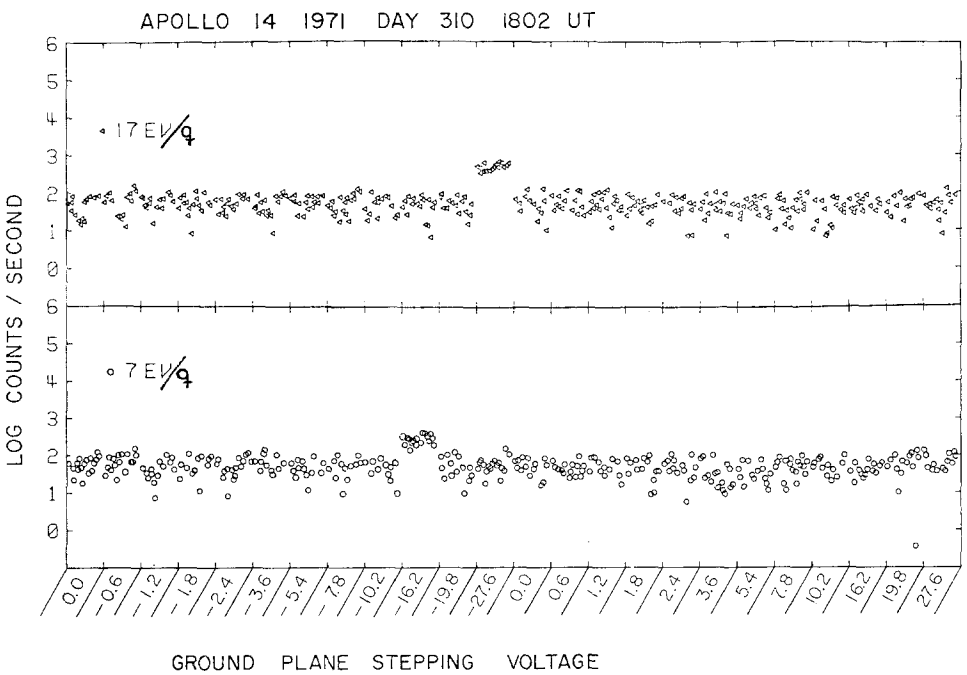

Fig. 4. Raw data from the SIDE differential energy channels as a function of ground plane stepper voltage (voltage of the SIDE relative to the ground plane).

plane stepping voltage. Figure 4 illustrates an example of these resonances in the actual raw SIDE count rate data. One can see a resonance in the 7 eV q^{-1} channel at the -16.2 ground plane stepping voltage, and another in the 17 eV q^{-1} channel, at the -27.6 ground plane stepping voltage. These two numbers taken together indicate a lunar surface potential of approximately $+10$ V at this particular time.

The overall results of the SIDE instrument lunar surface potential measurements

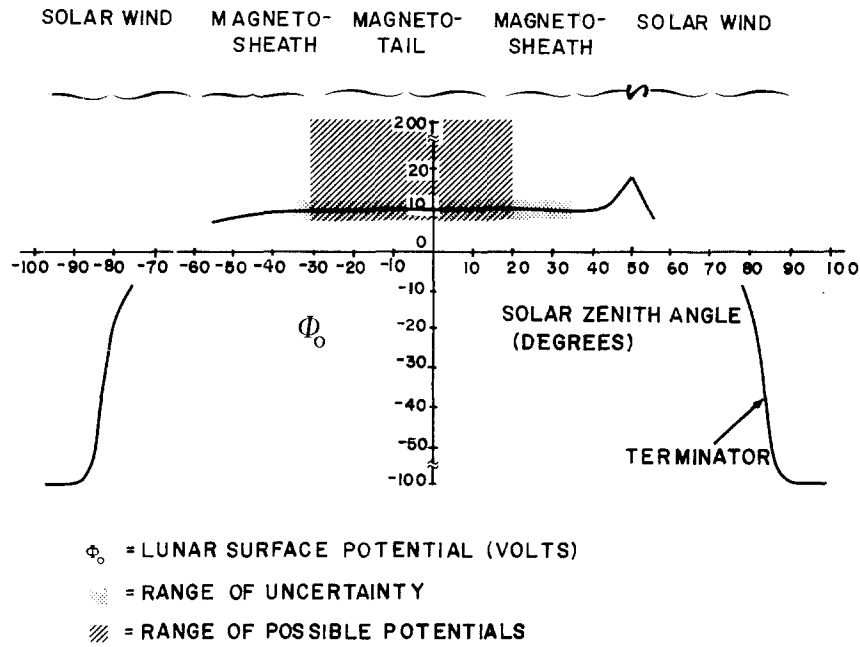

Fig. 5. The measured lunar surface potential, ϕ_0, as a function of solar zenith angle.

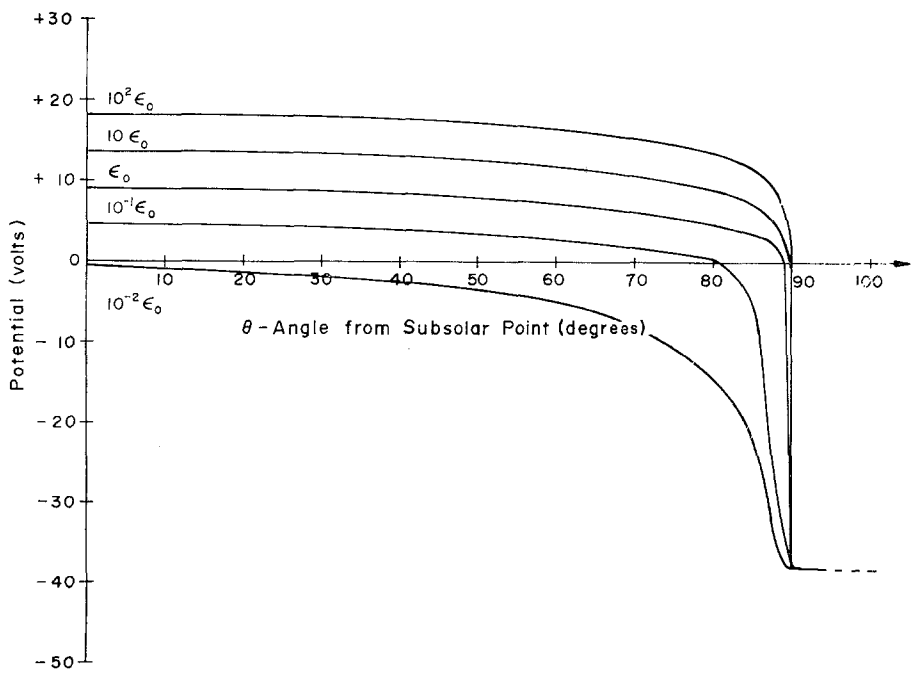

Fig. 6. Theoretical predictions of the lunar surface potential versus solar zenith angle prepared by Manka (1973). 'ε_0' is the emissivity corresponding to a photocurrent of 5×10^{-9} amp cm^{-2}.

are illustrated in Figure 5, on which we have plotted the electric potential on the lunar surface as a function of the solar zenith angle. For most of the late morning and early afternoon the lunar surface potential is in the vicinity of +10 V. A new result, reported here for the first time, is an asymmetry in this curve in the form of a small ear in the late lunar afternoon: the lunar surface potential rises to approximately +18 V. This effect is seen at the Apollo 15 site but not at the Apollo 14 site due to an instrumental effect.

Note, from Figure 5, that in early morning and late afternoon the surface potential goes to negative values as the terminator is approached. The potential measurements in these regimes are not made by the technique just described, but rather are derived from a set of data which will be described.

Goldstein (1974) has analyzed electron data from the ALSEP Solar Wind Spectrometer experiment and computed a lunar surface potential of the subsolar point in the solar wind of +5 to −3 V. The discrepancy between this result and the SIDE data has not yet been resolved.

Manka (1973) has investigated the lunar surface potential in the vicinity of the terminator regions. Figure 6 shows his theoretical curves indicating an asymptotic potential at the terminator of about −35 V. This value is highly dependent on the solar wind electron temperature and could in fact be considerably more negative at times. These theoretical curves bear a strong similarity to the observed potential curves shown in Figure 5.

Actual data on the lunar surface potential in the vicinity of the terminator can be obtained by the SIDE instrument through the observations of the atmospheric ions associated with the ion sheath adjacent to the lunar surface (Lindeman *et al.*, 1973). These ions reach the surface with peak energies corresponding to the lunar surface potential. As the SIDE approaches the terminator region very low energy ions are seen first. These energies increase gradually as the instrument passes the terminator. This phenomena is illustrated in Figure 7, where we see ions of approximately 10 eV about 1.5 days prior to the terminator. About 0.5 days before terminator crossing the ion energies begin to climb until they reach values of 70 eV approximately 0.5 days after the terminator crossing. This is believed to be a direct observation of the ambient lunar ions generated in the atmosphere by ultraviolet ionization and accelerated to the lunar surface by the negative surface potential. The energy in the ions is, therefore, a measurement of the lunar surface potential itself. Lindeman *et al.* (1973) have shown these potentials to go as low as −100 V on some terminator crossings. It is interesting to note that −70 V is about the potential expected for a *stationary* plasma whose ion and electron temperatures are 10^5 and 2×10^5 K, the temperatures appropriate to the solar wind. This calculation uses the potential expression given by Chopra (1961) for a body in a stationary plasma.

The fact that these ions are indeed ambient atmospheric ions is verified by some sample ion mass spectra also taken by the SIDE as shown in Figure 8.

The terminator electric potentials measured in this manner can be verified independently by the energy spectra of ions accelerated toward the moon by the *interplanetary*

electric field. These ions show the expected exponential spectra (Manka and Michel, 1973) offset by an amount of energy equal to that obtained in falling through the surface potential field. We thus have two independent determinations of the terminator surface potentials.

No theoretical studies have been published on the electric potential of the lunar

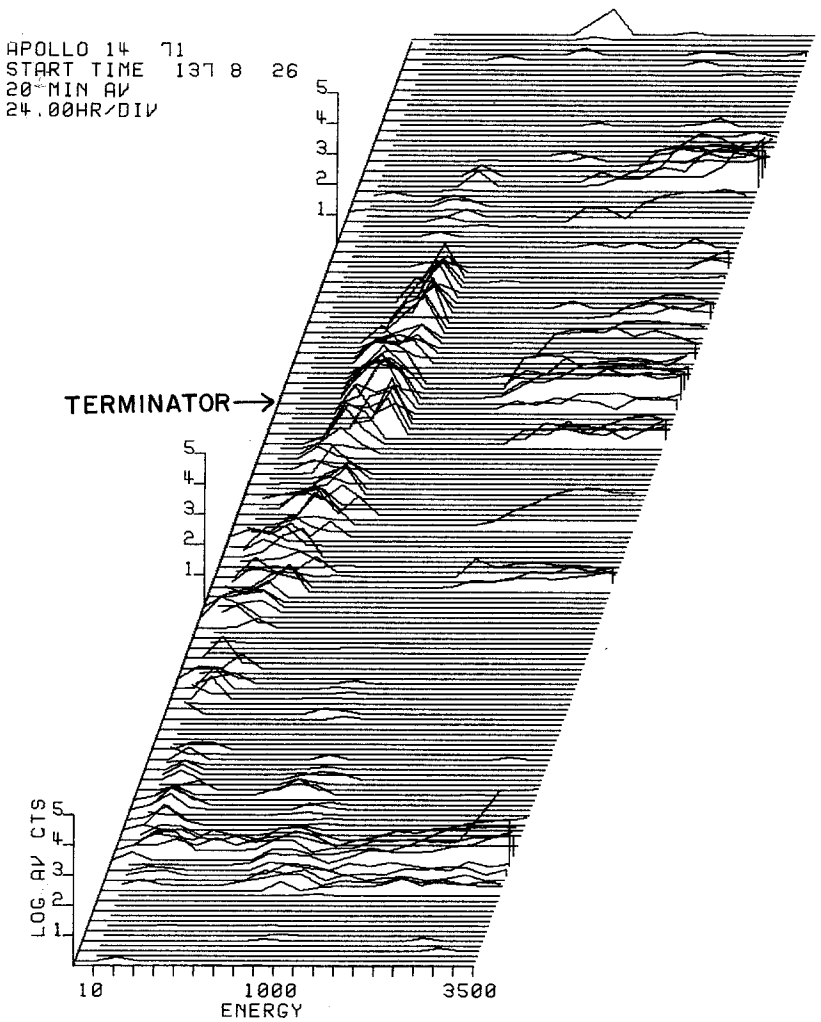

Fig. 7. SIDE total ion detector 20 minute average count rate energy spectra versus time. The start time is at the bottom of the figure and increases along the y-axis. The vertical log count scales are 24 hr apart. Energy along the x axis is in eV q^{-1}. The differential energy channels are as follows: 10, 20, 30, 50, 70, 100, 250, then increasing by 250 up to 3500 eV q^{-1}. Shortly after the start time at least three energy peaks are apparent. The lowest energy peak is due to ambient ions accelerated by the lunar surface potential. The peak at around 1000 eV q^{-1} may be turbulent solar wind whose flow has been disrupted by a limb shock. The higher energy peak, whose upper limit is outside our energy range, is due to protons escaping from the bow shock front of the Earth. These protons are seen on and off throughout this time period.

nightside and because of the absence of a strong ionizing mechanism our experimental techniques for the day and terminator regions are of no value here. A complete analysis of the problem involves a detailed study of the solar wind electron temperature and the ways, if any, in which it might be modified on the night side of the Moon.

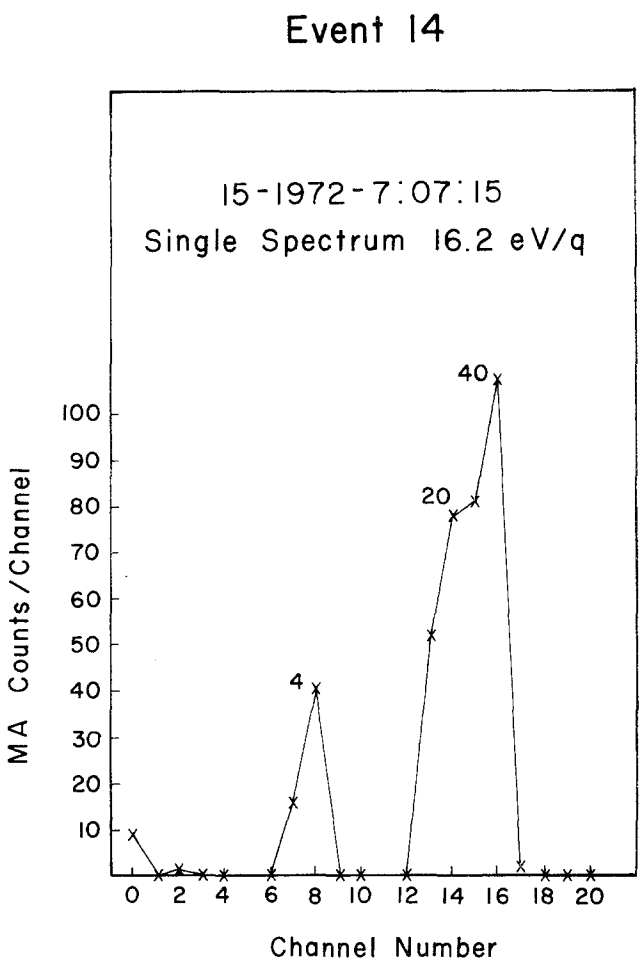

Fig. 8. A mass per unit charge spectrum from the SIDE mass analyzer showing three peaks tentatively attributed to helium, neon and argon. This spectrum, taken during a terminator crossing verifies that the low energy ions seen are from the lunar atmosphere and not accelerated solar-wind ions.

Reasoner (private communication) has CPLEE electron data which may prove helpful in this regard.

Schneider and Freeman (1974) and Freeman (1972) have reported ions of slightly less than solar wind energy whose flux is 2 orders of magnitude below that of the solar wind appearing on the night side of the Moon. These ions tend to occur most frequently several days before local sunrise and several days after sunset, however, they

have been seen throughout the entire lunar night. Whether or not these ions constitute a component of the lunar ionosphere remains to be seen. Certain $\mathbf{E}_{sw} \times \mathbf{B}_{sw}$ ion trajectories do allow transfer of atmospheric ions from the dayside to the nightside (Manka, private communication). The energy of the ions however suggests solar wind that has been diverted to the night side of the moon by some mechanism. One conceivable approach is to consider these ions to form the positive ion sheath for a negative nightside surface potential; in which case the deflecting force is electrostatic and the surface potentials required would be negative several hundred volts. We recall that the terminator nightside potential is indicated to be of the order of -100 V. Alternatively, these ions may arise from a turbulence or solar wind thermalizing process associated with limb shocks or the passage of the moon through the solar wind.

Next we direct our attention to the lunar surface potential in the geomagnetic tail.

Knott (1973) has pointed out that energetic electrons found in the plasma sheet can be expected to drive the nightside of the Moon to several kilovolts negative on occasions. Such large potentials are found on satellites in the tail during eclipses (DeForest, 1972).

Regarding the day side potential for the Moon in the geomagnetic tail, Reasoner and Burke (1972) have reported observations of photoelectrons in the photoelectron sheath whose cut-off energy indicate dayside potentials ranging up to approximately $+200$ V. Furthermore, they saw these potentials depressed to below their limit of detectability, $+40$ V, when the Moon entered the plasma sheet during an intense magnetic storm. The SIDE data show resonances, similar to those described above, in some regimes in the geomagnetic tail and indicates at those times potentials $+10$ V or greater. A detailed comparison of the SIDE and CPLEE data has not yet been made for periods of simultaneous data. It appears that the lunar surface potential can have a wide range of values in the tail depending on local plasma conditions. We expect more complete reports on tail potentials in the future. For completeness, the currently reported or predicted tail potentials are summarized in Table II.

Finally we discuss the electric fields associated with these surface potentials. For the photoelectron layer Walbridge (1973) calculates a field of the order of 10 to 15 V m^{-1}. This is consistent with our surface potential of 10 V if the effective screening length is 1 m. Feuerbacher *et al.* (1972) calculate 78 cm for the screening length.

TABLE II

Lunar surface potential in the tail

Workers	Method	Nightside	Dayside
Knott (1973)	From plasmasheet electron spectra	$\sim$ several kV in plasma sheet	
Reasoner and Burke (1972)	CPLEE photoelectron data		$\leqslant +40$ to $+200$ V
Freeman and Ibrahim	SIDE ion resonance data		$\geqslant +10$ V

In the terminator region we assume the Debye length to be that of the solar wind or approximately 10 m. Therefore, the electric field over the region where the surface potential can be determined by the SIDE is of the order of 1 to 10 V m^{-1} and directed radially inward.

The situation is much less certain on the far nightside. For the sake of completeness in this review we will *speculate* that the energetic ions ($N_0 \sim 0.05$ ion cm^{-3}) form an ion sheath for a surface potential of the order of -100 V, and that their effective temperature is that of the solar wind or $\sim 10^5$ K. In this case, the Debye length is of the order of 100 m and the electric field is 1 V m^{-1} directed radially inward.

Figure 2 summarizes the electric charge distribution around the Moon. The ion number densities shown, N_0, are those measured by the SIDE at the lunar surface. The ions forming the atmospheric ion sheath at the terminator are those illustrated in Figure 7. The nightside ions are those reported by Schneider and Freeman (1974).

Superimposed on the surface electric fields is the electric field of the solar wind whose value is of the order of 2×10^{-3} V m^{-1}. This field dominates any ion trajectory calculations at distances from the Moon greater than the Debye screening length.

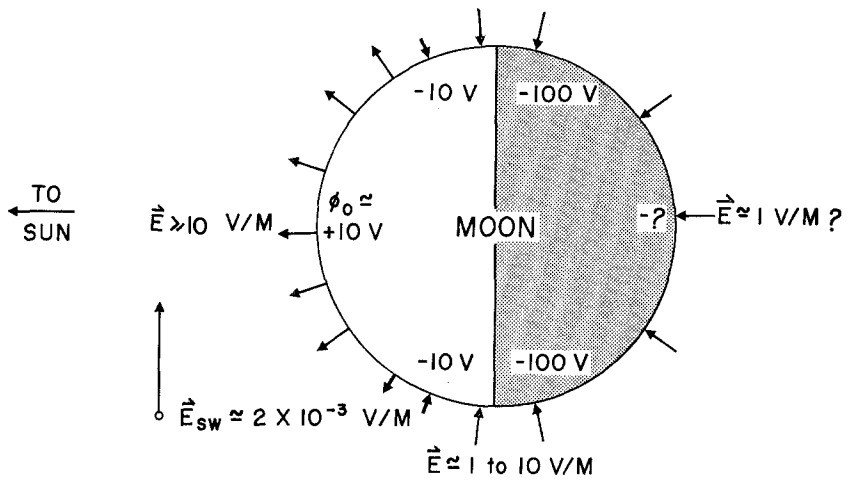

Fig. 9. The electric field environment of the Moon.

Figure 9 illustrates these electric field configurations. The electric fields considered in this paper are only large scale fields. As Criswell (1972, 1973) has pointed out small scale fields may be very intense.

Given these electric fields, it is possible to make calculations on the ion trajectories for ions arising from ionization of the lunar atmosphere. The results of these calculations are the subject of the paper by Vondrak and Freeman (1974). Similar calculations are also presented by Manka and Michel (1973).

In summary, the gross electric field distribution in the vicinity of the Moon is understood. The next task before us is to determine the effect of this electric field distribution on the lunar ionosphere. In this connection we note that only a small fraction of the

lunar atmosphere is found above the lunar surface at any time. The lunar atmosphere is essentially a solid state atmosphere residing beneath the lunar surface in the soil fines. This remarkable type of atmosphere is sustained, in part, by the ability of these electric fields to return ions to the surface with high velocities. We might say that the lunar atmosphere (at least for some gases) is recycled. Having established the electric field environment, it is now possible to proceed to consider quantitatively its effect on the ion return or reimplantation rates.

Acknowledgements

We gratefully acknowledge helpful discussions with many members of the Rice Space Physics and Astronomy Department, in particular Dr H. K. Hills and William J. Burke, and with D. R. Criswell of the Lunar Science Institute. This research was supported by NASA contract NAS9-5911.

References

Criswell, D. R.: 1972, *Geochim. Cosmochim. Acta.* **B**, *Suppl. 3*, 2671.
Criswell, D. R.: 1973, *The Moon* **7**, 202.
Chopra, K. P.: 1961, *Rev. Mod. Phys.* **33**, 153.
DeForest, S. E.: 1972, *J. Geophys. Res.* **77**, 651.
Feuerbacher, B., Anderegg, M., Fitton, B., Laude, L. D., and Willis, R. F.: 1972, *Geochim. Cosmochim. Acta, Suppl. 3*, **3**, 2655.
Freeman, J. W., Jr.: 1972, *J. Geophys. Res.* **77**, 239.
Freeman, J. W., Fenner, M. A., and Hills, H. K.: 1973, in R. J. L. Grard (ed.), *The Electric Potential of the Moon in the Solar Wind, Photon and Particles Interactions with Surfaces in Space*, D. Reidel Pub. Co., Dordrecht. See also *J. Geophys. Res.* (1973) **78**, 4560.
Goldstein, Bruce E.: 1974, *J. Geophys. Res.* **79**, 23.
Grobman, W. D. and Blank, J. L.: 1969, *J. Geophys. Res.* **74**, 3943.
Knott, K.: 1973, *J. Geophys. Res.* **78**, 3172.
Lindeman, R. A., Freeman, J. W., and Vondrak, R.: 1973, *Geochim. Cosmochim. Acta, Suppl. 3*, **3**, 2889.
Manka, Robert H.: 1973, in R. J. L. Grard (ed.), *Plasma and Potential at the Lunar Surface; Photon and Particle Interactions with Surfaces in Space*, D. Reidel Publ. Co., Dordrecht. See also R. H. Manka, *Geochim. Cosmochim. Acta, Supppl. 4*, **3** (1973), 2897.
Manka, R. H. and Michel, F. C.: 1973, *Geochim. Cosmochim. Acta, Suppl. 4*, **3**, 2897.
Öpik, E. J. and Singer, S. F.: 1960, *J. Geophys. Res.* **65**, 3068.
Reasoner, D. L. and Burke, W. J.: 1972, *J. Geophys. Res.* **77**, 6671. See also *J. Geophys. Res.* **78** (1973), 5844.
Schneider, H. E. and Freeman, J. W.: 1974, 'Energetic Lunar Nighttime Ion Events', Conference of Interactions of the Interplanetary Plasma with the Modern and Ancient Moon, Lake Geneva, Wisconsin, Cf. also *The Moon* **14**, 27, 1975.
Vondrak, R. R. and Freeman, J. W.: 1974, 'The Lunar Ionosphere', Conference on Interaction of the Interplanetary Plasma with the Modern and Ancient Moon, Lake Geneva, Wisconsin. Abstract volume available from the Lunar Science Institute, Houston, Texas 77058.
Walbridge, E.: 1973, *J. Geophys. Res.* **78**, 3668.